



1.1.3 HIERARCHICAL MODELING OF ACTIVE MATERIALS

Minoru Taya^{1*},
Professor and Director,
Center for Intelligent Materials and Systems
Department of Mechanical Engineering
University of Washington, Box 352600
Seattle, WA 98195-2600
U.S.A

Abstract

Intelligent (or smart) materials are increasingly becoming key materials for use in actuators and sensors. If an intelligent material is used as a sensor, it can be embedded in a variety of structure functioning as a health monitoring system to make their life longer with high reliability. If an intelligent material is used as an active material in an actuator, it plays a key role of making dynamic movement of the actuator under a set of stimuli.

This talk intends to cover two different active materials in actuators, (1) piezoelectric laminate with FGM microstructure, (2) ferromagnetic shape memory alloy (FSMA). The advantage of using the FGM piezo laminate is to enhance its fatigue life while maintaining large bending displacement, while that of use in FSMA is its fast actuation while providing a large force and stroke capability.

Use of hierarchical modeling of the above active materials is a key design step in optimizing its microstructure for enhancement of their performance. I will discuss briefly hierarchical modeling of the above two active materials. For FGM piezo laminate, we will use both micromechanical model and laminate theory, while for FSMA, the modeling interfacing nano-structure, microstructure and macro-behavior is discussed.

1. Introduction

Active Materials exhibit strains or property change upon a set of stimuli, thus ideal materials for use in sensors and actuators. This talk focuses only on the actuator materials. The scale of the actuators range from robotic arms to micron-sized MEMS. Design of new actuators with unique properties must cover the material design, actuator design and system design.

Hierarchical modeling of active materials is a key step in optimization of the microstructure of the active materials toward their best performance in use environment. The active materials that

* Corresponding author. Tel: 206-685-2850 Fax: 206-685-8047
E-mail address: tayam@u.washington.edu

are reviewed in this article are FGM piezoelectric composites and ferromagnetic shape memory alloys (FSMA).

Fig.1 illustrates popular active materials where (a) and (b) denote, respectively the stress-strain, and actuation time-strain relations for piezoceramics, shape memory alloys (SMAs) and electro-active polymers. The arrow sign in Fig.1. indicates the direction of improvement needed for these active materials.

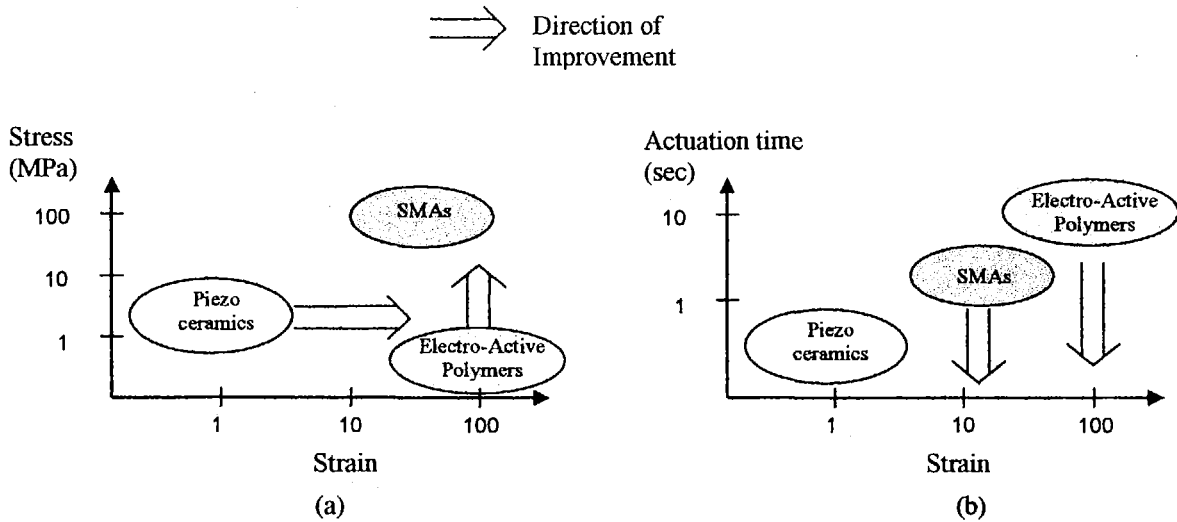


Fig. 1. Performance of three active materials, (a) range of stress and strain, (b) range of actuation speed and strain. The arrow sign denotes the direction of improvement in the performance of the active materials.

2. FGM Piezo Composites

The piezo actuators for bending mode are made of piezo monomorph bonded to a substrate, Fig. 2(a) or bimorph, Fig. 2(b) where the top and bottom piezo plate with identical piezo-elastic properties are bonded with opposite polarity such that the top expands while the bottom shrinks, thus providing bending mode displacement. Despite large bending displacement obtained by the bimorph piezo actuator, there exists a large stress field induced by the large misfit strain at the interface between the top and bottom plates, limiting the use life of the bimorph piezo actuator. The concept of functionally graded microstructure (FGM) was originally introduced to diffuse otherwise large thermal stress that exists at the interface between ceramic and metal plates which are bonded [1-3]. To reduce the induced stress field at the interface between the top and bottom plates in the bimorph piezo actuator, we proposed use of FGM [4].

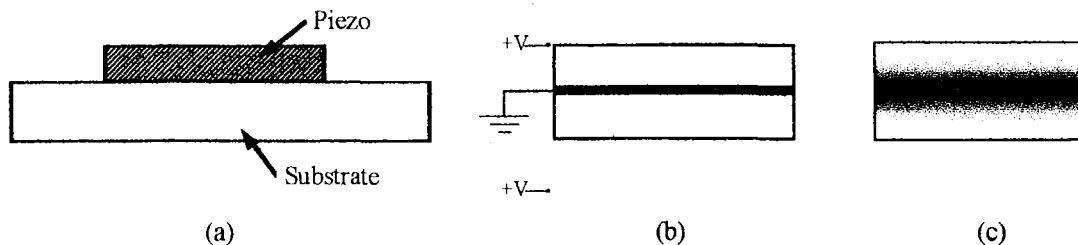


Fig. 2. Piezo actuators (a) monomorph (b) bimorph and (c) FGM bimorph

To tailor the optimum FGM layering, one needs to use a hierarchical modeling for such as FGM piezo composite actuator. The hierarchical modeling consists of (1) micromechanic model based on Eshelby's method [5, 6] and (2) laminate plate model [8, 9]. The micromechanic model is to predict the effective electroelastic properties of each lamina for a given set of constituent parameters (volume fraction of piezomaterials, their electroelastic properties, and shape). The detailed micromechanical modeling is described elsewhere [6,7] while a brief statement of the laminate plate model is given below.

The in-plane constitutive equations of a piezoelectric material of class 6mm type can be obtained from eq. (1) as

$$\begin{Bmatrix} \sigma_x \\ \sigma_y \\ \sigma_{xy} \end{Bmatrix}_i = \begin{bmatrix} \bar{Q}_{11} & \bar{Q}_{12} & 0 \\ \bar{Q}_{21} & \bar{Q}_{22} & 0 \\ 0 & 0 & Q_{66} \end{bmatrix}_i \begin{Bmatrix} \varepsilon_x^o + z\kappa_x - \alpha_{11}\Delta T \\ \varepsilon_y^o + z\kappa_y - \alpha_{11}\Delta T \\ \gamma_{xy}^o + z\kappa_{xy} \end{Bmatrix} - \begin{bmatrix} 0 & 0 & \bar{e}_{31} \\ 0 & 0 & \bar{e}_{32} \\ 0 & 0 & 0 \end{bmatrix}_i \begin{Bmatrix} 0 \\ 0 \\ E_z \end{Bmatrix}_i \quad (1)$$

where

$$\begin{aligned} \bar{Q}_{ij} &= C_{ij} - \frac{C_{i3}C_{j3}}{C_{33}} \\ \bar{e}_{ij} &= \frac{C_{j3}}{C_{33}}e_{33} - e_{ij} \end{aligned} \quad (2)$$

It is noted here that \bar{Q}_{ij} , \bar{e}_{ij} are the reduced stiffness constants and reduced piezoelectric constants that are modified by the assumption of plane stress and where $\varepsilon_x^o, \varepsilon_y^o$, and ε_{xy}^o are the in-plane strain components at mid-plane, $z = 0$, κ_x, κ_y , and κ_{xy} are the curvatures of the plate.

Each piezoelectric lamina is considered a capacitor whose electric field corresponds to its dielectric constant. The electric field in each layer of multi layer FGM piezoelectric can be obtained by considering the multi layers piezoelectric FGM as a series of condensers. The relationship between the electric capacity and the voltage is given as

$$C_i = \frac{Q}{V_i} \quad (3)$$

where C_i is the capacitance, Q is the charge, and V_i is the total voltage. The total capacitance in a series of capacitance is found as

$$\frac{1}{C_t} = \sum_{i=1}^n \frac{1}{C_i} = \sum_{i=1}^n \frac{d_i}{\varepsilon_i} \quad (4)$$

where d_i is the thickness of each capacitance or lamina as in piezoelectric FGM and ε_i is the dielectric constant for each lamina. The electric capacity in each layer will then be

$$C_i = \frac{Q}{V_i} = \frac{\varepsilon_i}{d_i} \quad (5)$$

Substituting eq.(3) and (4) into eq.(5) results in

$$V_i = Q \frac{d_i}{\varepsilon_i} = V_t \frac{d_i}{\varepsilon_i \sum_{l=1}^n \frac{d_l}{\varepsilon_l}} \quad (6)$$

The electric field in each layer can then be

$$E_i = \frac{V_i}{d_i} = V_t \frac{1}{\varepsilon_i \sum_{l=1}^n \frac{h_l - h_{l-1}}{\varepsilon_l}} \quad (7)$$

In-plane stress resultants (N_x, N_y, N_{xy}) and stress couples (M_x, M_y, M_{xy}) are defined as

$$\{N, M\} = \sum_{i=1}^n \int_{h_{i-1}}^{h_i} \{\sigma\} (dz, zdz) \quad (8)$$

Substituting eqs. (8) into (1), we obtain

$$\begin{bmatrix} N \\ M \end{bmatrix} = \begin{bmatrix} A & B \\ B & D \end{bmatrix} \begin{Bmatrix} \varepsilon^o \\ \kappa \end{Bmatrix} - \begin{bmatrix} N^E \\ M^E \end{bmatrix} \quad (9)$$

where

$$[A, B, D] = \sum_{i=1}^n \int_{h_{i-1}}^{h_i} [\bar{Q}] (dz, zdz, z^2 dz) \quad (10)$$

$$[N, M]^E = \sum_{i=1}^n \int_{h_{i-1}}^{h_i} [\bar{e}]_i \{E\}_i (dz, zdz) \quad (11)$$

In the above derivation, we assumed that the piezoelectric laminated plate is subjected to constant temperature and constant electric field. Under the constant applied electric field ($E_x = E_y = 0, E_z \neq 0$) and constant temperature ($\Delta T = 0$) in the absence of applied mechanical loading, we obtain from eq.(9) the strain of the mid-plane strain curvature as

$$\begin{bmatrix} \varepsilon^0 \\ \kappa \end{bmatrix} = \begin{bmatrix} a & b \\ b & d \end{bmatrix} \begin{bmatrix} N^E \\ M^E \end{bmatrix} \quad (12)$$

where

$$\begin{bmatrix} a & b \\ b & d \end{bmatrix} = \begin{bmatrix} A & B \\ B & D \end{bmatrix}^{-1} \quad (13)$$

The numerical results of the hierarchical modeling applied to standard bimorph (Fig. 2(b)) and the bimorph FGM of type A and B, see Fig.3 are listed in Table I.

Type of FGM microstructure	Standard bimorph, C91 Figure 7.2(a)	Standard bimorph, C6, Figure 7.2(a)	Bimorph FGM, C91-C6 Type B,	Bimorph FGM, C91-C6 Type A,
Applied Voltage (V)	33	33	33	33
Laminate thickness (mm)	0.67	0.67	0.67	0.67
No. of layers	2	2	6	6
Layer thickness (mm)	0.33	0.33	0.11	0.11
	PI = 0.01	PI = 0.01	PI = 0.01	PI = 0.01
Electric Field (V/mm)	100	100	100	100
Curvature (1/m)	0.152	0.102	0.143	0.112
Max. σ_x (MPa)	3.08	1.91	1.89	3.1
Deflection (μm) for plate length 50mm	47.5	31.9	44.8	29

Table I Comparison of out-of-plane displacement and in-plane stress in various types of piezo-composite plates

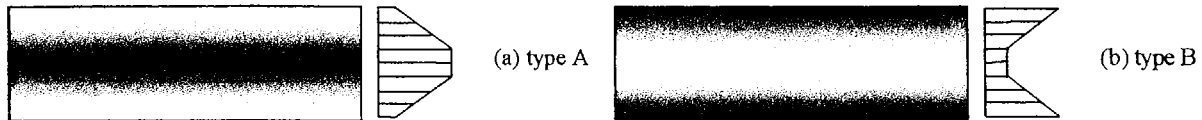


Fig. 3. Electroelastic properties distribution in FGM-bimorph

3. Hierarchical Modeling of Ferromagnetic Shape Memory Alloys (FSMA)

Since the pioneering work of Webster et al [5], there have been a number of works reported on ferromagnetic shape memory alloys (FSMA) with a promise of designing these into fast

responsive actuators. We proposed a new mechanism, “hybrid mechanism” which is a sequence of chair reaction; applied magnetic field gradient, magnetic force, stress-induced martensite phase transformation, softening of a FSMA, resulting in a large displacement [6]. We selected a polycrystalline FePd alloy as a promising FSMA as this alloy can be processed into any 3D shapes. To elucidate the proposed hybrid mechanism, we proposed a hierarchical modeling composed of nanomodel based on Bain Correspondent Varianto (BCV_s) and micromechanic model, Fig.4 [7].

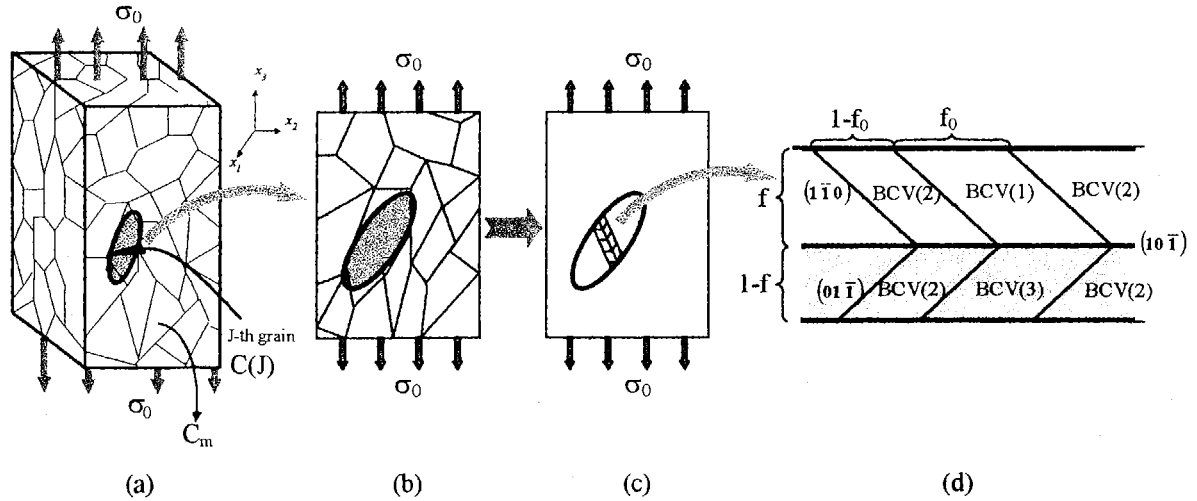


Fig.4 Hierarchical Modeling of Shape Memory Alloy (a) J-th grain embedded in a polycrystal with stiffness C_m , (b) J-th grain with $C(J)$ converted to (c) equivalent inclusion with C_m .

The nano-model is used to explain the nano-twin structure observed in a Fe-Pd alloy, Fig.4 (a) and Fig.5 (c). While the micromechanic model based on the micro-twin structure of Fig. 4 (b)-(c) is used to predict the stress strain curve of a polycrystalline Fe-Pd, Fig.6.

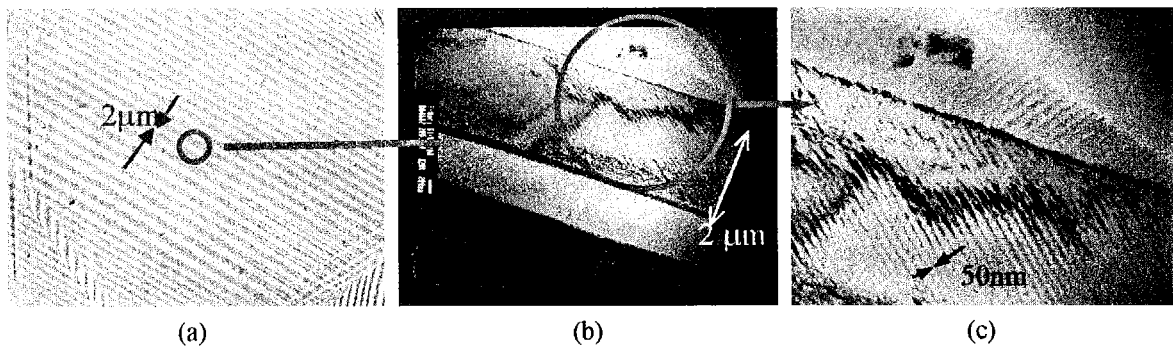


Fig.5 Structure of martensite in polycrystalline Fe-Pd (a) micro twins (b) nano twins (c)

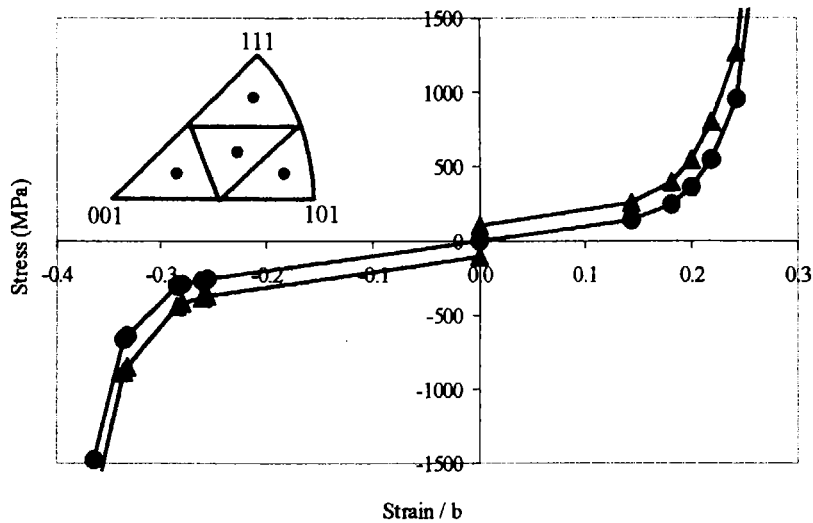


Fig. 6 Stress-strain curves of a polycrystalline Fe-Pd having 4 types of grains with (closed triangle) and without (closed circle) energy dissipation ($k = 2\text{MPa}$).

Acknowledgements

The author is thankful to the NEDO grant to the University of Washington on Smart Materials and Structures, and also to the Air Force Office of Scientific Research (F49620-02-1-0028).

References

- [1] A. Kawasaki, R. Watanabe, *J. Jpn Insti. Metal* **51**, 525-529 (1987).
- [2] M. Taya, J.K. Lee and T. Mori, *Acta Mater.*, **45**, 6, 2349-2356 (1997).
- [3] T. Hirai, Functionally gradient materials, in : R.J. Brook (Ed.), *Processing of Ceramics, Part 2, Materials Science and Technology*, vol. 17B, VCH, Weinheim, 293-341 (1996).
- [4] A. Almajid, M. Taya, S. Hudnut, *Int. J. Solids Struct.* **38**, 3377-3391 (2001).
- [5] P. J. Webster, K.R.A. Zrebeck, S.L. Town and M.S. Peak, *Phil. Mag.* **49**, 295- (1984).
- [6] H. Kato, T. Wada, T. Tagawa, Y. Liang, and M. Taya, *Proceedings of the 50th Anniversary of Japan Society of Materials Science*, Osaka, Japan, May 21-26, 296-305 (2001).
- [7] Y. Liang, T. Wada, T. Tagawa, and M. Taya, *Proceedings of SPIE Meeting*, San Diego, March 17-21, 2002, in press.